J HK Coll Radiol 2002;5:155-161

REVIEW ARTICLE

Imaging in Thalassaemia

YL Chan,[1] HY Tse[2]

[1]Department of Diagnostic Radiology and Organ Imaging, Prince of Wales Hospital, The Chinese University of Hong Kong, [2]Department of Obstetrics and Gynaecology, Kwong Wah Hospital, Hong Kong

ABSTRACT

Thalassaemia is the most important haemoglobinopathy in Hong Kong and Southeast Asia. In this review, the role of ultrasound in prenatal imaging of affected foetuses and the value of radiography and magnetic resonance imaging in the evaluation and management of thalassaemia are discussed.

Key Words: *Deferoxamine, Iron overload, Magnetic resonance imaging, Prenatal diagnosis, Thalassemia*

INTRODUCTION

Thalassaemia is the most important haemoglobinopathy in Hong Kong and Southeast Asia. In α-thalassaemia, the α-globin component of haemoglobin synthesis is defective. In β-thalassaemia the β-globin component of haemoglobin synthesis is affected. Imaging studies have a role in the diagnosis of this condition in different stages of life. They also have a role in the continuous monitoring and management of selected patients. In this review, the various aspects of imaging that could be of help in the diagnosis and management of thalassaemic patients are described.

α-THALASSAEMIA

In α-thalassaemia, mutation at the α-gene loci results in a defect of α-globin chain synthesis. Depending on the interaction and integrity of the paired gene loci in the 2 chromosomes, the phenotypic expressions include α-thalassaemia minor (trait), haemoglobin (Hb) H disease, and Hb Bart's hydrops foetalis. A mild,asymptomatic, haemolytic anaemia may be seen in α-thalassaemia trait, although there is no associated imaging abnormality, either during foetal or adult life. Red cell survival is reduced in Hb H disease due to haemolysis and there is also defective erythropoiesis. Approximately 70 to 80% of patients have hepatosplenomegaly. Extramedullary haematopoiesis that occurs is both mild and clinically insignificant. Likewise, iron overload is usually mild. Gallstones are frequently found.

Foetal haemoglobin is made up of 2 α-globin and 2 γ-globin chains. Hence, the deficient synthesis of α-globin chains in Hb Bart's disease is associated with a severe foetal anaemia that results in elevations of intrahepatic umbilical venous maximum flow velocity and middle cerebral artery peak flow velocity; both can be detected by Doppler US from 21 weeks of gestation onwards.[1] Echogenic bowel, thought to reflect hypoperistalsis or bowel wall oedema due to severe anaemia and hypoxia, is detected in 31% of affected foetuses between 12 and 24 weeks of gestation.[2]

The full-blown features of severe foetal hypoxia and heart failure include cardiomegaly, dilated umbilical vein, oedema, ascites, and pleural and pericardial effusion, all of which are readily demonstrated at US from 22 to 28 weeks of gestation onwards. Hb Bart's disease is the commonest cause of hydrops in Southeast Asia. Since these hydropic foetuses usually die in utero during the third trimester, both termination of pregnancy and, recently, in utero transfusion would be facilitated by early prenatal diagnosis. Timely management is also important in the case of pregnant mothers with prenatal complications in the form of pre-eclampsia or polyhydramnios, as well as post-partum mothers who experience massive haemorrhage from the enlarged placenta and/or sepsis.

Correspondence: *Dr. YL Chan, Department of Diagnostic Radiology and Organ Imaging, Prince of Wales Hospital, The Chinese University of Hong Kong, Shatin, Hong Kong.*
Tel: (852) 2632 1002; Fax: (852) 2636 0012;
E-mail: yl190chan@cuhk.edu.hk

Submitted: 3 June 2002; Accepted: 8 July 2002.

Early detection can be effectively achieved with US. The increase in placental thickness of affected foetuses occurs early in gestation. An increased placental thickness of more than 2 standard deviations (SDs) above the norm has been shown to be a sensitive sign of the disease, with a sensitivity of 72% before and 97% after 12 weeks of gestation.

The sign is positive in all affected foetuses after 18 weeks of gestation.[3] At a gestation of 18 to 21 weeks, a placental thickness of > 30 mm gives a sensitivity of 89%, a specificity of 90%, a positive-predictive value of 78%, and a negative-predictive value of 97% in diagnosing the condition (Figure 1a).[4] A cardiothoracic ratio cut-off of < 0.5 has been shown to identify 75% of affected pregnancies at 13 to 14 weeks of gestation, and all cases by 17 to 18 weeks of gestation (Figure 1b).[5]

US-guided chorionic villus biopsy, amniocentesis for DNA studies, and cordocentesis for foetal blood analysis are options for the definitive confirmation of Hb Bart's disease.

β-THALASSAEMIA

β-Thalassaemia is caused by mutations at the β-globin gene loci, resulting in defective output of β-globin chains. The main phenotypes are homozygous β-thalassaemia major, β-thalassaemia intermedia, and β-thalassaemia minor. Although a mild degree of ineffective erythropoiesis may be found in β-thalassaemia minor, no imaging abnormalities are present. As its name would suggest, β-thalassaemia intermedia, which is due to the interaction of many different thalassaemia alleles, has a variable clinical picture between that of β-thalassaemia minor and β-thalassaemia major.[6]

Since homozygous β-thalassaemia major is a disorder of β-globin synthesis, foetal haemoglobin production is not affected. Foetuses with the disorder appear normal physiologically and at imaging studies. Rather, the role of imaging is in the provision of US-guided prenatal diagnostic procedures, namely, chorionic villus sampling and amniocentesis, which are established procedures at different times of the gestation period to obtain foetal DNA for diagnosis.

Production of γ-globin chains declines after birth and the compromised β-globin chain production in homozygous β-thalassaemia major leads to the premature death of red cells. Without treatment, severe anaemia and death ensue in early childhood. Blood transfusion is the standard treatment for homozygous β-thalassaemia major and, during the past 20 years, has improved both the quality of life and life expectancy of these patients. The clinical and imaging picture of the patient depends on the adequacy of transfusion, the amount of blood transfused, and the chelation therapy applied.

Inadequate Transfusion

Untreated or undertreated thalassaemia results in marked red marrow hyperplasia[7] accompanied by characteristic radiographic features of medullary expansion.[8] In the skull, this manifests as widening of the diploic space, and a typical 'hair on end' appearance may be seen in severe cases. Rarefaction and cortical thinning are seen in the spine, ribs, and long bones.[9-12]

Non-skeletal manifestations of thalassaemia include extramedullary haematopoiesis, haemosiderosis, splenomegaly, and cholelithiasis. Due to sequestration and/or an increased transfusion requirement, hypersplenism

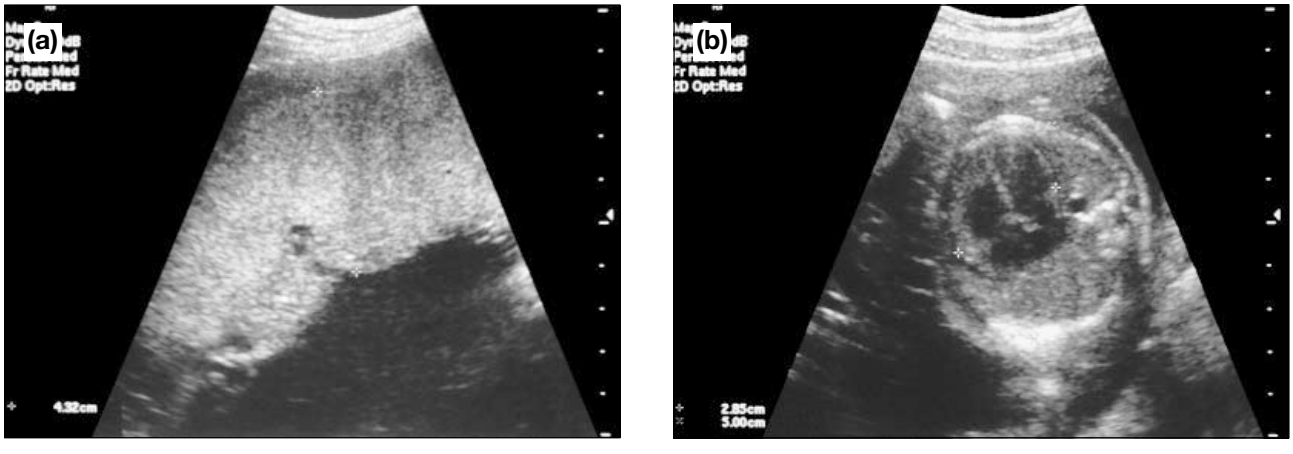

Figure 1. Ultrasound of a 22-week 6-day-old foetus with homozygous α-thalassaemia. (a) The placenta is enlarged, with a thickness increased to 4.3 cm; (b) sectional image through the thorax of the foetus pertaining to a 4-chamber view of the heart . At 57%, the cardiothoracic ratio (ratio of the dimension of the heart across the atrio-ventricular valves and the transverse diameter of the thorax) is increased.

may develop and consequently thrombocytopenia. Partial splenic-embolisation has been employed as an alternative to splenectomy in alleviating hypersplenism in children with thalassaemia.[13] Extramedullary haematopoiesis is most commonly detected in the paraspinal region as soft tissue masses on plain radiography, CT or MRI. At MRI, iron deposition or fatty replacement may also be seen in older inactive masses.[14]

Rarely, intraspinal extension of extramedullary haematopoiesis may lead to cord compression. Due to the longer survival of patients with homozygous β-thalassaemia, the problem of cholelithiasis is becoming more frequent. Its incidence increases with age and occurs in more than 80% of patients older than 31 years, according to a review of 48 patients by Goldfarb et al.[15] Patients with anaemia may develop cardiomegaly and signs of cardiac decompensation, the onset of which may be rapid.

Adequate Transfusion

In 1989, Scutellari et al observed a decrease of the classic radiographic findings due to medullary expansion in hypertransfused β-thalassaemia patients compared with low-transfused patients.[16] The current authors have only observed radiographic evidence of medullary expansion in patients who spent their childhood outside Hong Kong undergoing irregular transfusion.[17] Contemporary blood transfusion regimens effectively eliminate radiographic evidence of marrow expansion, although other radiographic abnormalities are observed.

Osteoporosis

Papageorgiou et al showed that 91% of hyptertransfused patients with β-thalassaemia major developed osteoporosis and 70% developed cortical thinning.[18] In addition, decreased bone mineral density has been documented on dual energy X-ray absorptiometry.[19,20] De Vernejoul et al, observed thin metacarpal cortices related to increased resorption in patients with thalassaemia major with Hb maintained at 10 g/dL.[21] 41% of patients receiving regular transfusion had thinned metacarpal cortex to 2 SDs below the normal mean.[17] Such osteoporosis is reportedly associated with vertebral fracture and bone pain.[22] The aetiology of osteoporosis is probably multifactorial: hypogonadism, hormonal activity affecting bone remodelling, and persistently elevated erythropoietic activity have all been implicated.[17,22-24]

Growth Failure and Bone Age Delay

Growth retardation in patients with β-thalassaemia major is probably multifactorial, and may be caused by inadequate transfusion, iron overload with hypothalamic pituitary function derrangement, and/or deferoxamine toxicity.[6,7,23] Short stature is primarily due to a decrease in sitting height, which, in turn, is related to deferoxamine toxicity on spinal growth resulting in platyspondyly (flattened vertebral bodies). Bone age delay is characteristic and may be related to the delay in pubertal spurt.

Iron Overload

Iron overload in undertransfused patients is the result of both transfusion iron loading and increased iron absorption, whereas in adequately transfused patients it is due primarily to transfusion loading. In the latter, excess iron is harmlessly stored in reticuloendothelial cells of the bone marrow, spleen, and liver by the process of haemosiderosis. The liver is the largest of these stores and the hepatic iron overload reflects the total body iron overload. More harmful forms of iron deposition occur with increases in iron loading that saturate the capacity of the reticuloendothelial system. In the liver, hepatic parenchymal injury results in fibrosis and cirrhosis, although the latter is more commonly due to transfusion-related hepatitis.

The pancreas is also affected in severe iron overload; this accounts for the higher incidence of diabetes mellitus that is observed. The affected pancreas is markedly hypointense on MRI, in a manner similar to haemochromatosis. In the heart, myocardial iron loading results in heart failure and death due to cardiac failure; cardiac toxicity remains the most common cause of mortality in patients with thalassaemia.[25] The risk of cardiac disease and early death is greatly increased when the liver iron concentration exceeds 15 mg/g dry weight.[26] Toxic iron storage in the hypothalamic-pituitary axis is thought to result in hypothalamic-pituitary dysfunction and hypogonadism. Despite the absence of abnormal pulmonary radiographic findings, respiratory abnormalities may be detected in patients with thalassaemia major, of which impairment of diffusion capacity is the commonest. Li et al found no correlation between respiratory function impairment and body iron content in thalassaemia major patients.[27]

Serum ferritin concentration is a convenient and commonly used marker of total body iron content. However, it is affected by haemolysis, ineffective erythropoiesis, inflammation, and liver disease, and its accuracy in the estimation of body iron under these circumstances has been shown to be unreliable.[28-30]

Liver iron content gives a more reliable estimation of the total body iron content.[29-31] The assessment of liver iron concentration in thalassaemia major patients receiving regular transfusion is important in the adjustment of deferoxamine dosage to avoid undertreatment, with a risk of cardiac and liver toxicity, and overtreatment, with a risk of deferoxamine toxicity. It can be determined quantitatively by atomic absorption spectrophotometry on tissue cores obtained from liver biopsy.[32] Atomic absorption spectrophotometry, however, is labour-intensive, technique-demanding, and does not have widespread availability. Moreover, a discrepancy between atomic absorption spectrophotometry and histological grading for the estimation of liver iron concentration in biopsy samples has been reported.[33] In this regard, variation in the regional liver iron concentration[34,35] may influence how representative the small liver biopsy sample is.[33] Although quantitative liver iron measurement can be achieved non-invasively using super conducting quantum interference, this technique has a restricted availability.[36]

Magnetic resonance imaging employing short echo times (TE) to measure T2-relaxation time is accurate in the estimation of liver iron content.[37-39] The shortest TE employed determines the highest iron level that can be accurately quantified.[40] However, using a TE as low as 10 ms (with a multi-echo technique capable of measuring T2-relaxation time) may not be feasible with all commercially-available MRI scanners due to a limitation in the gradient switch time.[41,42] On the other hand, measuring the signal intensity of the liver to paraspinal muscle (L/M) ratio on T1-weighted images is a simpler method that can be performed on all MRI machines. Although the estimate of liver iron concentration from the L/M ratio is only moderately accurate,[33] clinically important thresholds can be established from the ratios. It has been shown that all patients with an L/M ratio of < 0.6 have histological iron storage grade 3 or 4, which approximates to 7.3 to 47.4 mg/g dry weight. Accordingly, a threshold L/M ratio of < 0.6 will help identify most patients at higher risk of iron toxicity, that is those who have a liver iron concentration > 15 mg/g dry weight (Figure 2).[33]

Recently, assessment of the myocardial iron load from T2-star relaxation time measurement on MRI has been reported.[43] Since cardiac toxicity from iron overload is the most important factor affecting survival in thalassaemia major patients, this method will impact on the appropriate chelation dose and perhaps also the choice of whether to use deferoxamine, an oral chelator, or a combination of both.

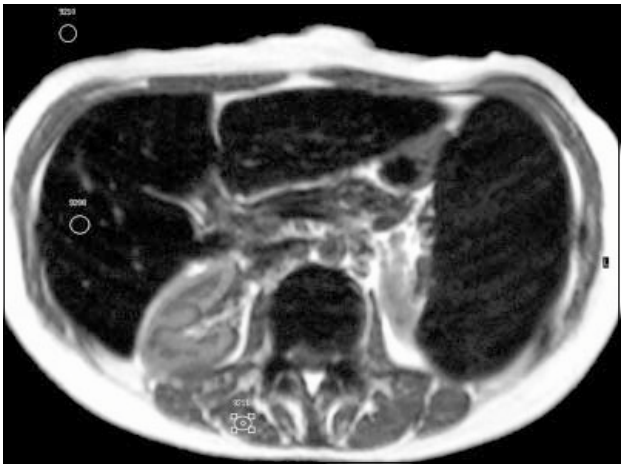

Figure 2. Axial T1-weighted spin-echo (TR/TE 550/15) image of the abdomen of a 22-year-old woman transfused since the age of 2 years and chelated since the age of 4 years, with an unsatisfactory compliance to chelation therapy. The liver parenchyma is markedly hypointense with a L/M ratio of 0.2.

Complications of Chelation Therapy

Standard therapy of iron overload is by subcutaneous injection of the chelator deferoxamine. While insufficient chelation carries the risk of iron toxicity to the heart, liver, and endocrine organs, overchelation may lead to deferoxamine-induced dysplastic changes in the long bones, which is associated with short stature.[44-49] In a cross-sectional study of 35 patients with thalassaemia major, 12 (34%) had evidence of deferoxamine-induced bone dysplasia on hand radiographs obtained for the assessment of skeletal age.[49]

Garofalo et al reported a much higher incidence (85%) of skeletal dysplasia with metaphyseal bone thickening and vertebral flattening in 23 patients receiving regular transfusion and chelation.[20] Although the risk of dysplasia increases with high-dose chelation therapy (> 50 mg/kg/day) commenced at an early age (< 3 years),[44] the balance between deferoxamine level and the amount of iron available for chelation may be more important. Seven of 12 patients (58%) with radiographic evidence of deferoxamine-induced bone dysplasia had chelation started at or after 3 years of age with a dose not exceeding 50 mg/kg/day.[49]

Radiographic features of deferoxamine-induced dysplasia have been well documented.[17,44-51] Typically, this complication involves the metaphysis of the most actively growing part of the long bones.[17,45-47,50] Metaphyseal sclerotic and lucent foci at the fast growing distal

Figure 3. Plain radiograph of the right knee of a 13-year-old girl chelated since the age of 3 years. Blurring of the physeal-metaphyseal junction and metaphyseal sclerosis (open arrow) are noted at the distal femur. The sclerotic change extends just a short distance away from the proximal tibial physes (lower black arrow), but in the distal femur it reaches the metadiaphyseal region (upper black arrow). Mild lucency with a sclerotic rim (small black arrow) is noted at the metaphysis of the proximal fibula.

radius and ulna, distal femur and proximal tibia, and fibula are characteristic features. The growth plate may be widened. The metaphyseal changes, as they migrate with growth, become angular or irregular sclerotic stripes at the metadiaphyses,[48] which are therefore markers of previous deferoxamine-induced injury (Figure 3).

Often, asymptomatic dysplastic changes may be detected on radiographs of the left hand obtained for bone age estimation, as well as chest radiographs obtained for cardiac assessment. These radiographs should therefore be carefully scrutinised at the tubular bones of the hand, wrist, the proximal humerus, and the ribs. Genu valgum is frequently associated with a dysplastic change at the knee, which may be so severe as to require corrective surgery.[46-50] Platyspondyly is also a dysplastic feature[51] that may account for the truncal shortening in these patients. Routine spinal radiography for the detection of platyspondyly has been recommended as part of the monitoring process in deferoxamine-induced bone dysplasia.[51]

A significant association exists between long bone dysplasia and continuing height reduction.[46,47,49] Olivieri et al noted that patients with more marked metaphyseal lesions had the most severe height reduction.[46] The mechanism whereby deferoxamine affects bone growth is not entirely clear, but may involve chelation of zinc[44,45] and an anti-proliferative effect of the drug.[52-57] Early detection of the condition is important, since reducing the deferoxamine dose has been shown not only to reverse the bone abnormality, but also to improve bone growth.[45,47]

Radiographic evidence of bone dysplasia, however, lags behind pronounced growth failure by 2 to 3 years.[48] MRI capable of imaging cartilage and delineating

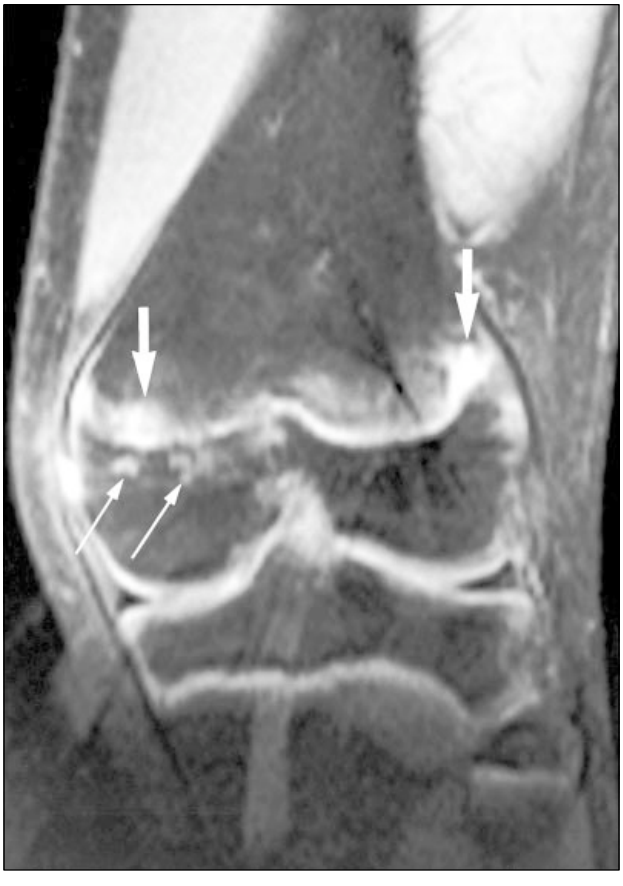

Figure 4. A 15-year-old male chelated since the age of 6 years. Coronal fat-saturated proton density (TR/TE 2000/11) image of the left knee shows metaphyseal hyperintensity, which is particularly marked at the periphery (arrows). Juxtaphyseal epiphyseal hyper intense foci are also seen (thin arrows).

physeal and metaphyseal lesions[58,59] is a more sensitive technique in the diagnosis of deferoxamine-induced bone dysplasia.[60] Besides metaphyseal changes, lesions are also detected in the epiphysis, physis, and metadiaphyseal region on MRI. The peripheral (especially lateral) predominance of all the following changes is well delineated on fat-saturated proton density-weighted MRI: physeal widening; blurred physeal-metaphyseal junction; juxtaphyseal hyperintensity at the distal metaphysis; and metadiaphyseal serpiginous or linear hypointensities (Figure 4).[60] This technique thus has the capacity to provide early detection of the complication of deferoxamine-induced skeletal dysplasia.

Notching at the metaphyseal corner, blurred or irregular peripheral juxtaphyseal metaphyseal contour, and widening of the peripheral juxtaphyseal metaphyseal echogenic interface are sonographic signs of deferoxamine-induced dysplasia. However, although specific, US is only modestly sensitive as a diagnostic modality and mild dysplasia may evade detection.[61] Its role may therefore be confined to the assessment of severe dysplastic changes.

SUMMARY

Imaging support, including plain radiography, US, CT, and MRI, has a role in assisting the diagnosis and/or management of patients with thalassaemia. This is defined by the type of haemoglobinopathy (α-thalassaemia or β-thalassaemia), the phenotype, the stage and age of the patient, and the treatment.

REFERENCES

1. Leung WC, Oepkes D, Seaward G, Ryan G. Serial sonographic findings of four fetuses with homozygous alpha-thalassemia-1 from 21 weeks onwards. Ultrasound Obstet Gynecol 2002;19: 56-59.
2. Lam YH, Tang MH, Lee CP, Tse HY. Echogenic bowel in fetuses with homozygous alpha-thalassemia-1 in the first and second trimesters. Ultrasound Obstet Gynecol 1999;14:180-182.
3. Ghosh A, Tang MH, Lam YH, Fung E, Chan V. Ultrasound measurement of placental thickness to detect pregnancies affected by homozygous alpha-thalassaemia-1. Lancet 1994;344:988-989.
4. Tongsong T, Wanapirak C, Sirichotiyakul S. Placental thickness at mid-pregnancy as a predictor of Hb Bart's disease. Prenat Diagn 1999;19:1027-1030.
5. Lam YH, Ghosh A, Tang MH, Lee CP, Sin SY. Early ultrasound prediction of pregnancies affected by homozygous alpha-thalassaemia-1. Prenat Diagn 1997;17:327-332.
6. Olivieri NF, Weatherall DJ. Clinical aspects of β-thalassemia. In: Disorders of haemoglobin: genetics, pathophysiology, and clinical management. In: Steinberg MH, Forget BG, Higgs DR, Nagel RL, eds. Cambridge: Cambridge University Press; 2001: 277-341.
7. Rioja L, Girot R, Garabedian M, Cournot-Witmer C. Bone disease in children with homozygous β-thalassemia. Bone Miner 1990;8:69-86.
8. Resnick D. Hemoglobinopathies and other anemias. In: Resnick D, Diagnosis of bone and joint disorders, 3rd ed. Philadelphia: WB Saunders; 1995:2107-2146.
9. Tunaci M, Tunaci A, Engin G, et al. Imaging features of thalassemia. European Radiol 1999;9:1804-1809.
10. Pootrakul P, Hungspregnes S, Fucharoen S, et al. Relation between erythropoiesis and bone metabolism in thalassemia. New Engl J Med 1981;304:1470-1473.
11. Lawson JP, Ablow RC, Pearson HA. Calvarial and phalangeal vascular impresions in thalasemia. AJR Am J Roentgerol 1984; 143:641-645.
12. Orzincolo C, Castaldi G, Bariani L, Franceschini F, Corcione, Scutellari PN. Circumscribed lytic lesions of the thalassaemic skull. Skeletal Radiol 1988;17:344-347.
13. Stanley P, Shen TC. Partial embolization of the spleen in patients with thalassemia. J Vasc Intervent Radiol 1995;6:137-142.
14. Tsitouridis J, Stamos S, Hassapopoulou E, Tsitouridis K, Nikolopoulos P. Extramedullary paraspinal hematopoiesis in thalassemia: CT and MRI evaluation. Eur J Radiol 1999;30:33-38.
15. Goldfarb A, Grisaru D, Gimmon Z, Okon E, Lebensart P, Rachmilewitz EA. High incidence of cholelithiasis in older patients with homozygous beta-thalassemia. Acta Haematol 1990; 83:120-122.
16. Scutellari PN, Orzincolo C, Franceschini F, Bagni B. The radiographic appearances following adequate transfusion in β-thalassaemia. Skeletal Radiol 1989;17:545-550.
17. Chan YL, Pang LM, Chik KW, Cheng JCY, Li CK. Patterns of bone diseases in transfusion-dependent homozygous β-thalassaemia major — predominance of osteoporosis and deferoxamine-induced bone dysplasia. Pediatr Radiol 2002. In press.
18. Papageorgiou O, Papanastasiou DA, Beratis NG, Korovessis P, Oikonomopoulos A. Scoliosis in β-thalassemia. Pediatrics 1991; 88:341-345.
19. Goni MH, Markussis V, Tolis G. Bone mineral content by single- and dual-photon absorptiometry in thalassemic patients. In: Ando S, Brancati C, eds. Endocrine disorders in thalassemia, Berlin:Springer-Verlag; 1995:47-51.
20. Garofalo F, Piga A, Lala R, Chiabotto S, Di Stefano M, Isaia GC. Bone metabolism in thalassemia. Ann NY Acad Sci 1998;850: 475-478.
21. De Vernejoul MC, Girot R, Gueris J, et al. Calcium phosphate metabolism and bone disease in patients with homozygous thalassemia. J Clin Endocrinol Metab 1982;54:276-281.
22 Giardina P. Osteoporosis in thalassemia. Abstracts of the 8th international conference on thalassemia and the hemoglobinopathies, Athens, Greece, 2001:48-50.
23. Lala R, Chiabotto P, Di Stefano M, Isaia GC, Garofalo F, Piga A. Bone density and metabolism in thalassaemia. Journal Pediat Endocrinol Metab 1998;11(Suppl 3):785-790.
24. Pootrakul P, Hungspregnes S, Fucharoen S, et al. Relation between erythropoiesis and bone metabolism in thalassemia. New Engl J Med 1981;304:1470-1473.
25. Olivieri NF, Brittenham GM. Iron chelating therapy and the treatment of thalassemia. Blood 1997;89:739-761.
26. Brittenham GM, Grifith PM, Nienhius AW, et al. Efficacy of deferoxamine in preventing complications of iron overload in patients with thalassemia major. N Engl J Med 1994;331:567-573.
27. Li AM, Chan D, Li CK, Wong E, Chan YL, Fok TK. Respiratory function in patients with thalassaemia major — relationship with iron overload. Arch Dis Child 2002. In press.

28. Brittenham GM, Cohen AR, McLaren CE, et al. Hepatic iron stores and plasma ferritin concentration in patients with sickle cell anemia and thalassemia major. Am J Hematol 1993;42:81-85.
29. Rocchi E, Cassanelli M, Borghi A, et al. Magnetic resonance imaging and different levels of iron overload in chronic liver disease. Hepatology 1993;17:1997-2002.
30. Pippard MJ. Measurement of iron status. Prog Clin Biol Res 1989;309:85-92.
31. Angelucci E, Giardini C, Brittenham GM, Lucarelli G. Hepatic iron concentration and body iron stores determined by quantitative phlebotomy in patients cured of thalassemia major by bone marrow transplantation. Blood 1997;90(Suppl 1):265a.
32. Angelucci E, Baronciani D, Lucarelli G, et al. Needle liver biopsy in thalassaemia: analyses of diagnostic accuracy and safety in 1184 consecutive biopsies. Br J Haematol 1995;89: 757-761.
33. Chan YL, Li CK, Lam CW, et al. Liver iron estimation in beta-thalassaemia: comparison of MRI biochemical assay and histological grading. Clin Radiol 2001;56:911-916.
34. van Deursen C, de Metz M, Koudstaal J, Brombacher P. Accumulation of iron and iron compounds in liver tissue. A comparative study of the histological and chemical estimation of liver iron. J Clin Chem Biochem 1988;26;617-622.
35. Ambu R, Crisponi G, Sciot R, et al. Uneven hepatic iron and phosphorus distribution in beta-thalassemia. J Hepatol 1995; 23:544-549.
36. Fischer R, Tiemann CD, Engelhardt R, et al. Assessment of iron stores in children with transfusion siderosis by biomagnetic liver susceptometry. Am J Hematol 1999;60:289-299.
37. Rocchi E, Cassanelli M, Borghi A, et al. Magnetic resonance imaging and different levels of iron overload in chronic liver disease. Hepatology 1993;17:1997-2002.
38. Gomori JM, Horev G, Tamary H, et al. Hepatic iron overload: quantitative MR imaging. Radiology 1991;179:367-369.
39. Papakonstantinou OG, Maris TG, Kostaridou V, et al. Assessment of liver iron overload by T2-quantitative magnetic resonance imaging: correlation of T2-QMRI measurements with serum ferritin concentration and histologic grading of siderosis. Magn Reson Imaging 1995;13:967-977.
40. Engelhardt R, Langkowski JH, Fischer R, et al. Liver iron quantification: studies in aqueous iron solutions, iron overloaded rats, and patients with hereditary hemochromatosis. Magn Reson Imaging 1994;12:999-1007.
41. Ernst O, Sergent G, Bonvarlet P, Canva-Delcambre V, Paris JC, L'Hermine C. Hepatic iron overload: diagnosis and quantification with MR imaging. AJR Am J Roentgerol 1997;168: 1205-1208.
42. Angelucci E, Giovagnoni A, Valeri G, et al. Limitations of magnetic resonance imaging in measurement of hepatic iron. Blood 1997;90:4736-4742.
43. Anderson LJ, Holden S, Davis B, et al. Cardiovascular T2-star (T2*) magnetic resonance for the early diagnosis of myocardial iron overload. Eur Heart J 2001;22:2171-2179.
44. De Virgilis S, Congia M, Frau F, et al. Deferoxamine-induced growth retardation in patients with thalassemia major. J Pediatr 1988;113:661-669.
45. Brill PW, Winchester P, Giardina PJ, Cunningham-Rundles S. Deferoxamine-induced bone dysplasia in patients with thalassemia major. AJR Am J Roentgerol 1991;156:561-565.
46. Olivieri NF, Koren G, Harris J, et al. Growth failure and bony changes induced by deferoxamine. Am J Pediatr Hematol Oncol 1992;14:48-56.
47. Orzincolo C, Scutellari PN, Castaldi G. Growth plate injury of the long bones in treated b-thalassemia. Skeletal Radiol 1992; 21:39-44.
48. De Sanctis V, Pinamonti A, Di Palma A, et al. Growth and development in thalassaemia major patients with severe bone lesions due to desferrioxamine. Eur J Pediatr 1996;155:368-372.
49. Chan YL, Li CK, Pang LM, Chik KW. Desferrioxamine-induced long bone changes in thalassaemic patients — radiographic features, prevalance and relations with growth. Clin Radiol 2000; 55:610-614.
50. Naselli A, Vignolo M, Di Battista, et al. Long-term follow-up of skeletal dysplasia in thalassaemia major. J Pediatr Endocrin Metab 1998;3:817-825.
51. Hartkamp MJ, Babyn PS, Olivieri F. Spinal deformities in deferoxamine-treated homozygous beta-thalassemia major patients. Pediatr Radiol 1993;23:525-528.
52. Estrov Z, Tawa A, Wang XH, et al. In vitro and in vivo effects of deferoxamine in neonatal acute leukemia. Blood 1987;69: 757-761.
53. Iwata M, Zager RA. Myoglobin inhibits proliferation of cultured human proximal tubular (HK-2) cells. Kidney Int 1996; 50:796-804.
54. Kaplinsky C, Estrov Z, Freedman MH, Gelfand EW, Cohen A. Effect of deferoxamine on DNA synthesis, DNA repair, cell proliferation, and differentiation of HL-60 cells. Leukemia 1987; 1:437-441.
55. Lederman HM, Cohen A, Lee JV, Freedman M, Gelfand EV. Deferoxamine: a reversible S-phase inhibitor of human lymphocyte proliferation. Blood 1984;64:748-753.
56. Tzanno-Martins C, Naves ML, Elorriaga R, Fraga PM, Jorgetti V, Cannata JB. Evaluating the effect of desferrioxamine on bone cell proliferation. Nephrol Dial Transplant 1995;10:714-715.
57. Tomoyasu S, Fukuchi K, Yajima K, et al. Suppression of HL-60 cell proliferation by desferrioxamine: changes in c-myc expression. Anticancer Res 1993;13:407-410.
58. Laor T, Jaramillo D. Metaphyseal abnormalities in children: pathophysiology and radiologic appearance. AJR Am J Roentgerol 1993;161:1029-1036.
59. Laor T, Jaramillo D, Hoffer FA, et al. MR imaging in congenital lower limb deformities. Pediatric Radiol 1996;26:381-387.
60. Chan YL, Li CK, Chu WCW, Pang LM, Cheng JCY, Chik KW. Deferoxamine-induced bone dysplasia in the distal femur and patella of pediatric patients and young adults: MR imaging appearance. AJR Am J Roentgerol 2000;175:1561-1566.
61. Chan YL, Chu CW, Chik KW, Pang LM, Shing MK, Li CK. Deferoxamine-induced dysplasia of the knee: sonographic features and diagnostic performance compared with magnetic resonance imaging. J Ultrasound Med 2001;20:723-728.